Polyhedron 115 (2016) 17–29

Contents lists available at ScienceDirect

Polyhedron

journal homepage: www.elsevier.com/locate/poly

Ti, Zr and V complexes with N-allyl functionalized heterocyclic ligands as catalysts for ethylene polymerization

Hamdi Ali Elagab, Helmut G. Alt *

Laboratorium für Anorganische Chemie, Universität Bayreuth, Postfach 10 12 51, D-95440 Bayreuth, Germany

ARTICLE INFO

Article history:
Received 18 March 2016
Accepted 12 April 2016
Available online 30 April 2016

Dedicated to Professor Max Herberhold on the occasion of his 80th birthday (August 02, 2016).

Keywords:
Ti, Zr, V complexes
N-allyl functionalized heterocyclic ligands
Catalytic ethylene polymerization
Multimodal resins
Single-reactor technology

ABSTRACT

Titanium, zirconium and vanadium complexes with N-allyl functionalized 1,2-bis(benzimidazolyl)benzene, 1,2-bis(benzimidazolyl)ethane, 1,1-bis(benzimidazolyl)methane, 2,2-bis(benzimidazolyl), 2,6-bis(benzimidazolyl)pyridine and 2-(benzimidazolyl)pyridine ligands were synthesized and characterized. After activation with methylaluminoxane (MAO) they were applied for catalytic ethylene polymerization. The performance of such homogeneous catalysts is unique: they have high activities (up to 3278 kg PE/mol cat h), they produce bimodal or multimodal resins with high molecular weights and they have the potential to produce their own support for heterogeneous polymerization reactions. Such catalysts combine all features for single-reactor bimodal polyethylene technology.

1. Introduction

In industrial polyethylene production the applied catalyst [1–5] is the most important component in the process. A catalyst should not only perform with high activity, it should also be heterogeneous in order to avoid fouling in the reactor and it should produce bimodal or multimodal resins for advantageous processing. A perfectly designed catalyst should be able to combine all these qualifications and produce the desired product in one step and in one reactor. In the past, our group afforded good progress with such intelligent catalysts [6] and we found solutions to this problem with self-immobilizing catalysts [7–11] and bi- or multinuclear catalysts [12–15]. Now we could improve and simplify this approach with mononuclear complexes carrying heterocyclic ligands. Recently we reported the preparation and characterization of 1,2-bis(benzimidazoles) and 2,6-bis(benzimidazolyl) pyridine compounds and their titanium, zirconium and vanadium complexes [16]. One surprising result in catalytic ethylene polymerization was the fact that some of these mononuclear complexes, after activation with methylaluminoxane (MAO), produced bimodal or multimodal resins [17]. We explained this result with different interaction modes of the bulky MAO anion and the hetero atoms in the catalyst cation. Now only one more step was necessary to make such catalysts heterogeneous and for this reason alkenyl groups should be introduced into benzimidazole complexes in order to provide self-immobilization potential of the homogeneous catalyst without using any support. So far, in the literature the synthesis of 2,6-bis(N-allyl benzimidazolyl)pyridine copper(II) complexes, N-alkylated 2-(benzimidazolyl)pyridine and 2,6-bis(benzimidazolyl)pyridine chromium(III) complexes have been described in ethylene polymerization and oligomerization reactions [18–20]. Herein, the preparation and characterization of N-allyl substituted 2-(benzimidazolyl)pyridine, 1,2-bis(benzimidazolyl)benzene, 1,2-bis(benzimidazolyl)ethane 1,1-bis(benzimidazolyl)methane, 2,2-bis(benzimidazolyl) and 2,6-bis(benzimidazolyl)pyridine along with their titanium, zirconium and vanadium complexes and their use in ethylene polymerization reactions after activation with methylaluminoxane is reported.

2. Results and discussion

2.1. Synthesis of bis(benzimidazoles) and the 2-benzimidazolyl pyridine compounds **1**–**6**

The condensation reaction of a dicarboxylic acid or an acid anhydride in preheated polyphosphoric acid with a diamine is a well established procedure for the preparation of the imidazole based ligand precursors **1**–**6** [21,22] in high yields (Scheme 1).

---

* Corresponding author. Tel.: +49 921 43864.
E-mail address: helmut.alt@uni-bayreuth.de (H.G. Alt).

http://dx.doi.org/10.1016/j.poly.2016.04.014
0277-5387/

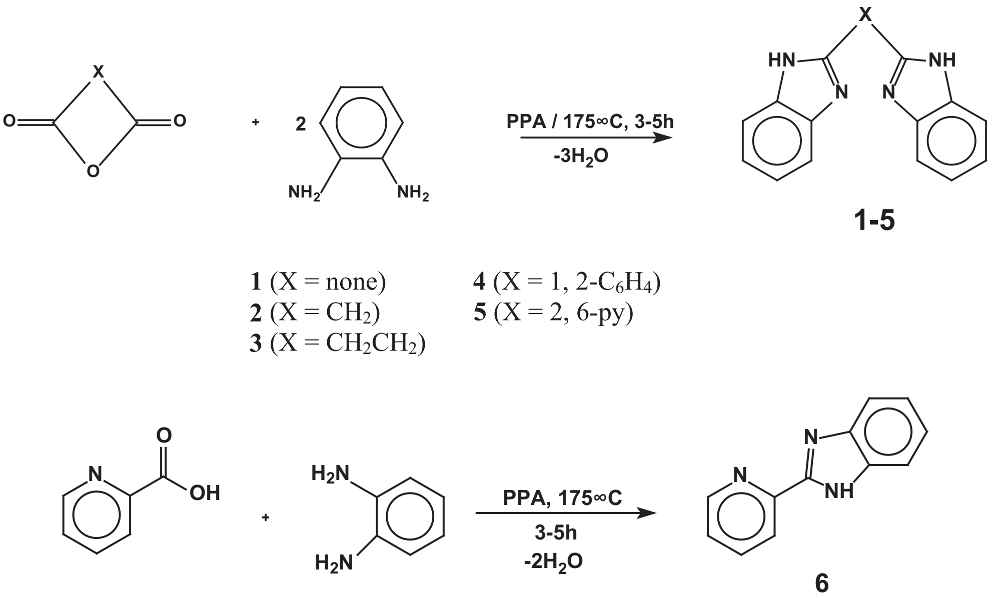

Scheme 1. Synthesis of the bis (benzimidazolyl) compounds **1**–**5** and 2-benzimidazolyl pyridine (**6**).

2.2. Synthesis of the allyl substituted imidazoles ***7–12***

N-allyl substituted bis-benzimidazoles were prepared according to a published procedure [23]. In the presence of potassium carbonate, the N-allylation proceeded readily to give the desired product in aprotic solvents, especially DMF under mild conditions. However, the reaction of allyl bromide with 2-(benzimidazolyl) pyridine is more productive. Generally, the introduction of one allyl group is much easier compared with double allylation. This is clearly shown from the yield of each reaction under the same conditions (Scheme 2).

2.3. Synthesis of transition metal complexes ***13–44***

The complexes **13**–**44** were synthesized according to Schemes 3 and 4 by mixing the THF adducts of titanium or zirconium tetrachloride in dichloromethane with the ligand precursors under constant stirring for 24 h. The vanadium complexes were prepared

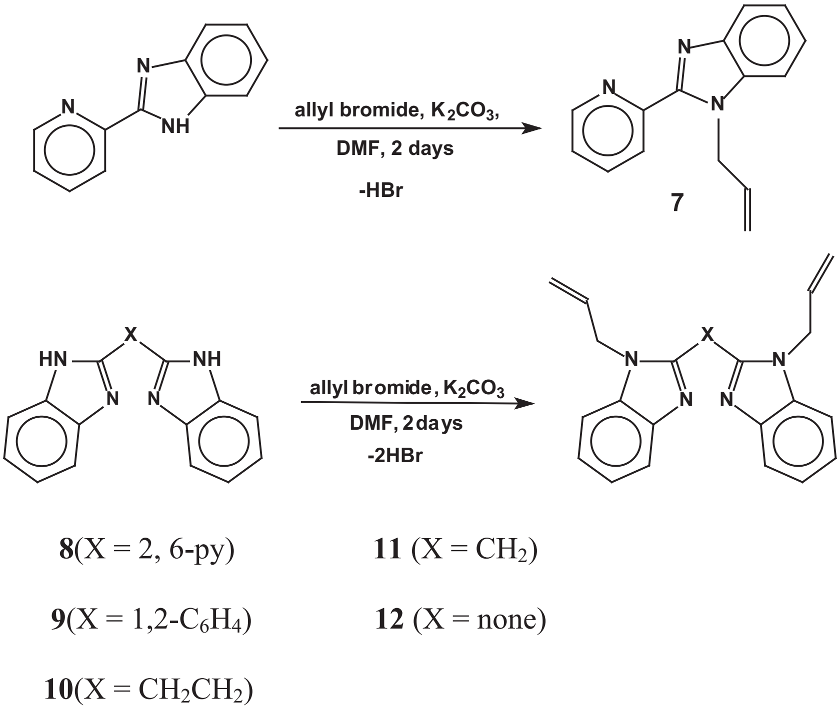

Scheme 2. Synthesis of the ligand precursors **7**–**12**.

16-28 **13-15**

Complex No	Bridging unit X	M
13		Ti
14		Zr
15		V
16	2,6-Py	V
17	1,2-Ph	Ti
18	1,2-Ph	Zr
19	1,2-Ph	V
20	CH_2CH_2	Ti
21	CH_2CH_2	Zr
22	CH_2CH_2	V
23	CH_2	Ti
24	CH_2	Zr
25	CH_2	V
26	-	Ti
27	-	Zr
28	-	V

Scheme 3. Synthesized bis-benzimidazole and 2-benzimidazolyl pyridine complexes **13**–**28**.

similarly using diethyl ether as solvent. They were precipitated quantitatively.

2.4. Characterization

2.4.1. NMR spectroscopy

The organic compounds **1**–**12** and transition metal complexes **13**–**44** were characterized by ^1H NMR and ^{13}C NMR spectroscopy in addition to elemental analysis of representative samples.

The ^1H NMR spectrum of compound **7** (Fig. 1) shows ten sets of resonance signals. H1 and H4 appear as doublets at $\delta = 8.64$ [$^3J_{H,H} = 5.4$ Hz] and 8.38 ppm ($^3J_{H,H} = 7.9$ Hz). The pseudo triplet at $\delta = 7.83$ ppm ($^3J_{H,H} = 7.9$ Hz) is assigned to H3. H5 and H8 give doublets at $\delta = 7.75$ and 7.42 ppm.H2, H6 and H7 appear as superimposed multiplets in the range of $\delta = 7.37$–7.23 ppm. A quartet of doublets in the region of $\delta = 6.12$–6.02 ppm represents the CH proton H10 of the allyl group coupling with the cis and trans protons of H11 and the two protons of H9. A doublet at $\delta = 5.52$ ppm ($^3J_{H,H} = 5.4$ Hz) corresponds to the methylene protons H9. A doublet of doublets at $\delta = 5.07$ ppm ($^3J_{H,H} = 6.8$ and 12.5 Hz) corresponds to the protons of the terminal CH_2 group of the double bond at H11.

The ^{13}C NMR spectrum of compound **7** (Fig. 2) shows 15 resonance signals each equivalent to one carbon atom of the molecule. The signals at $\delta = 150.9$, 150.0, 148.8, 143.0, 137.4, 137.0, 133.9, 124.7, 124.0, 123.4, 122.6, 120.1, 116.6, 110.9 and 48.2 ppm are assigned to C5, C12, C11, C1, C6, C3, C14, C2, C8, C4, C9, C10, C15, C7 and C13.

The ^1H NMR spectrum of complex **30** (Fig. 3) shows ten sets of resonance signals. H1 and H4 give doublets at $\delta = 8.88$ [$^3J_{H,H} = 5.4$ Hz] and 8.62 ppm ($^3J_{H,H} = 7.9$ Hz). The virtual triplet at $\delta = 8.21$ ppm ($^3J_{H,H} = 7.9$ Hz) is assigned to H3. The two multiplets at $\delta = 8.00$ and 7.92 ppm are an AA‘BB’ pattern and can be assigned to H6 and H7. A doublet of doublets at $\delta = 7.73$ ppm ($J_{H,H} = 5.4$ Hz) is assigned to H2. Two superimposed doublets at $\delta = 7.61$ ppm correspond to H5 and H8. The quartet of doublets at $\delta = 6.16$–6.03 ppm represents the CH proton of the allyl group (H10). A doublet at $\delta = 5.60$ ppm ($J_{H,H} = 5.4$ Hz) corresponds to the methylene protons H9. The doublet of doublets at $\delta = 5.22$ ppm originates from the terminal CH_2 group (H11) of the double bond.

The ^{13}C NMR spectrum of complex **30** (Fig. 4) shows 15 resonance signals each equivalent to one carbon atom of the molecule. The signals at $\delta = 151.1$, 146.8, 144.1, 139.1, 134.0, 132.9, 132.4, 127.7, 127.4, 127.1, 127.0, 119.5, 116.0, 114.6 and 49.1 ppm are assigned to C5, C12, C11, C1, C6, C3, C14, C2, C8, C4, C9, C10, C15, C7 and C13.

2.4.2. Mass spectrometry

The mass spectrum of compound **7** (Fig. 5) shows the molecular ion peak ($M^{\circ+}$) with $m/z = 234$. The peak with $m/z = 195$ represents the loss of the allyl group ($M^{\circ+}$–allyl).

The mass spectrum of complex **30** (Fig. 6) shows the ion resulting from the loss of the allyl group at $m/z = 425$. The ion with $m/z = 396$ represents the loss of two chlorides. The loss of three chlorides results in an ion with $m/z = 361$. Finally, at $m/z = 235$, an ion of the free ligand appears.

2.5. Polymerization results

All coordination compounds were activated with MAO and we assume a mechanism which is in agreement with that proposed for the activation of metallocene [24,25] and 2,6-bis(imino)pyridine iron(II) [26] catalyst precursors. The high molecular weight of the polymers indicate that the rate of propagation reactions (the activation barrier for propagation is usually low if existent at all) [27,28] are much faster than the rate of termination (the termination reactions are subjected to activation barriers).

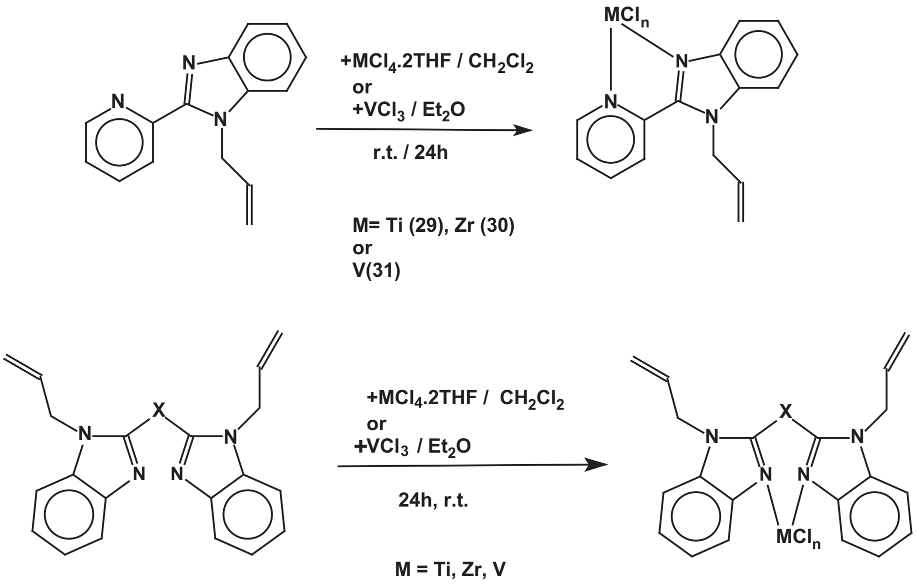

Complex No.	Bridging unit (X)	M
29		Ti
30		Zr
31		V
32	2,6-py	V
33	1,2-Ph	Ti
34	1,2-Ph	Zr
35	1,2-Ph	V
36	CH_2CH_2	Ti
37	CH_2CH_2	Zr
38	CH_2CH_2	V
39	CH_2	Ti
40	CH_2	Zr
41	CH_2	V
42	-	Ti
43	-	Zr
44	-	V

Scheme 4. Synthesis of the N-allyl-substituted transition metal complexes **29**–**44**.

The polymerization activities of N-allyl-2-benzimidazolyl pyridine titanium, zirconium, and vanadium complexes were investigated (Table 1). The vanadium catalyst **31**/MAO showed the highest activity (3279 [kg PE/mol cat h]) compared to the titanium catalyst **29**/MAO (433 [kg PE/mol cat h]) and the zirconium catalyst **30**/MAO (167 [kg PE/mol cat h]). Since all parameters are the same, it must be the metal, that makes the difference, presumably because of very low activation energies in the various polymerization steps such as ethylene insertion into the metal polymer chain. We had observed a similar behaviour earlier, when our research group tested complexes with identical compositions but with different transition metals for catalytic ethylene oligomerization and polymerization [25,26]. The 2,6-bis(benzimidazolyl)pyridine vanadium catalyst **32**/MAO showed an activity of 118 [kg PE/mol cat h] (Fig. 7).

In comparison to the systems without an allyl substituent (**13**, **14** and **15**) the activities were greatly enhanced by its introduction. The reason is not so obvious and we can only speculate. The allyl group is increasing the electrophilicity of the metal centre and hence the Lewis acidity of the active center. But this effect should not contribute to such a high degree. It is more likely that the allyl group can stabilize intermediates intramolecularly in the various polymerization steps as indicated earlier. An advantageous interaction with the MAO counter anion can also be considered. The polymerization activities of 1,2-bis(N-allyl-benzimidazolyl)benzene, 1,2-bis(N-allyl-benzimidazolyl)ethane,1,1-bis(N-allyl-benzimidazolyl)methane and bis-benzimidazolyl titanium, zirconium and vanadium complexes compared to the unsubstituted complexes containing N–H groups were greatly affected by the N-allyl substituents. The unsubstituted catalysts **17**–**28**/MAO show relatively

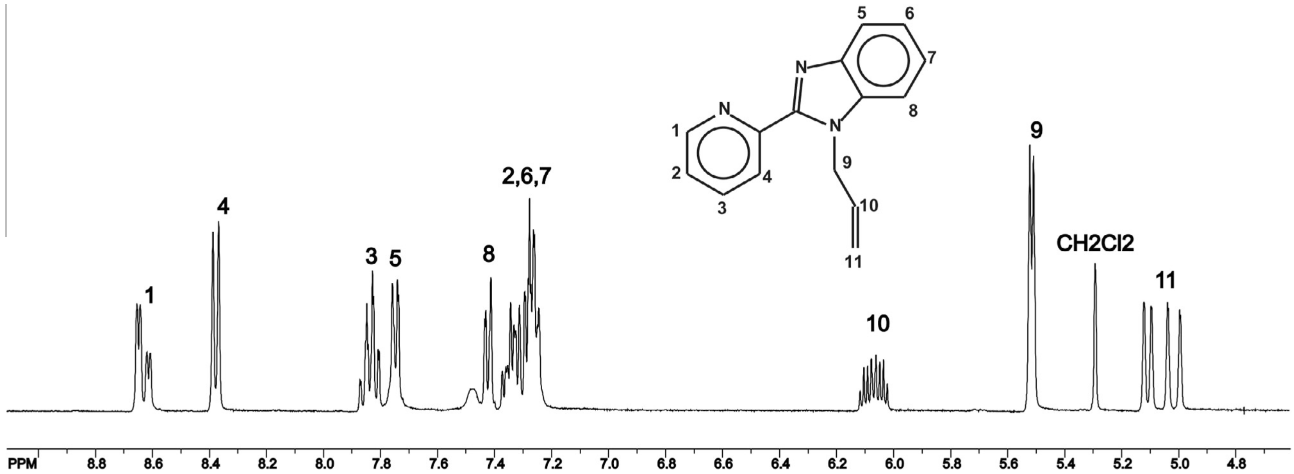

Fig. 1. ^{1}H NMR spectrum of compound **7** in CD_2Cl_2.

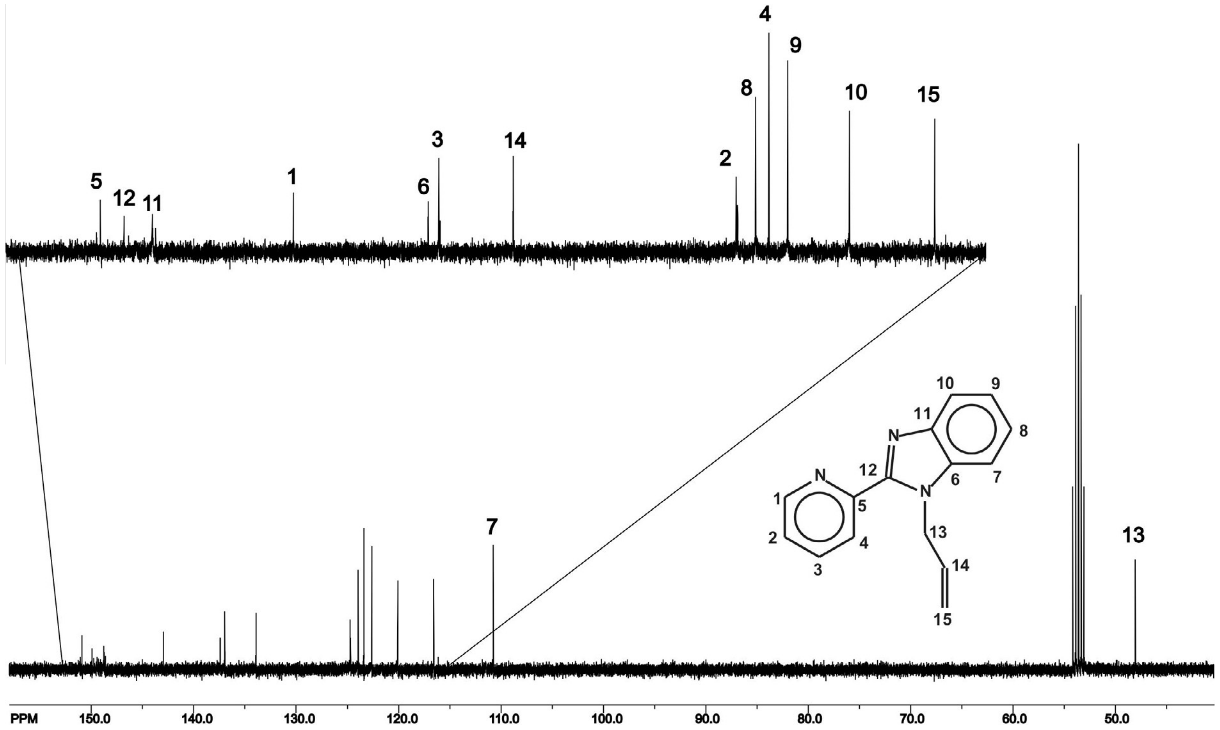

Fig. 2. ^{13}C NMR spectrum of compound **7** in CD_2Cl_2.

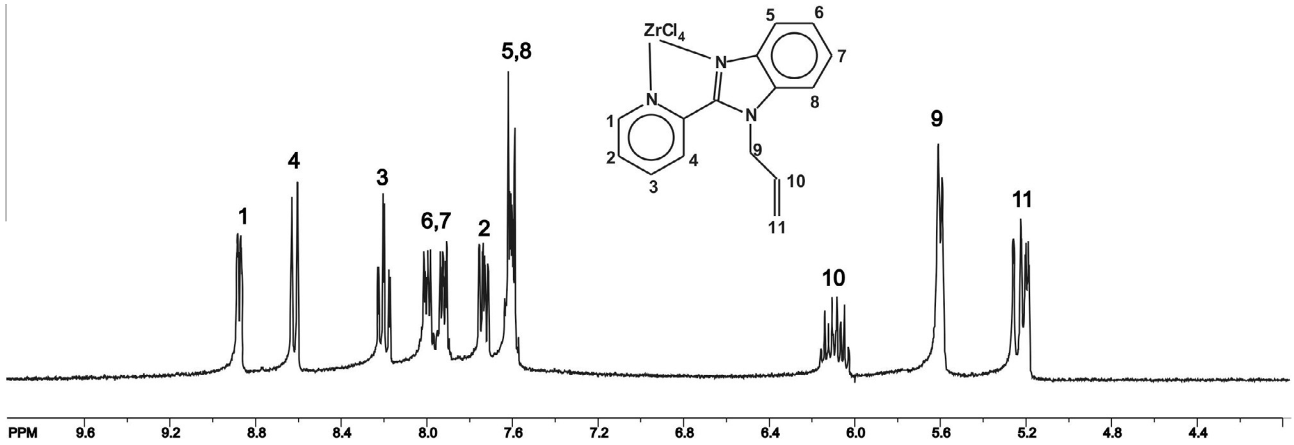

Fig. 3. ^{1}H NMR spectrum of complex **30** in DMSO-d_6.

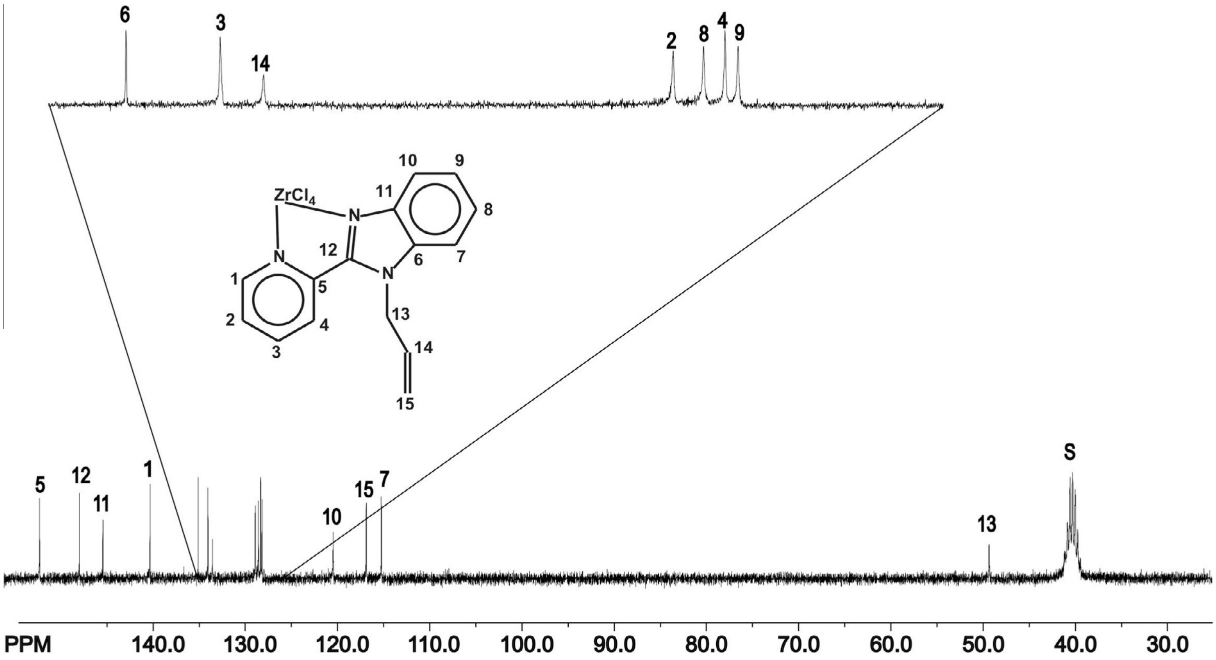

Fig. 4. ^{13}C NMR spectrum of complex **30** in DMSO-d_6.

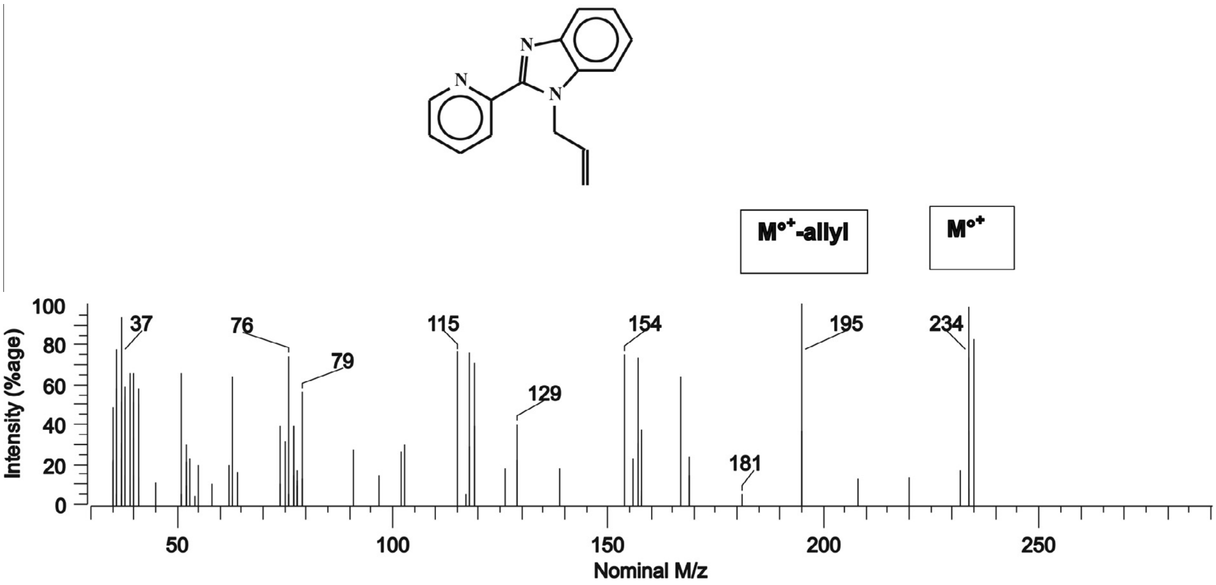

Fig. 5. Mass spectrum of compound **7**.

high catalytic activities compared to the N-allyl substituted analogues (Fig. 8). This could possibly be caused by their deprotonation to give anionic amide ligands when activated with MAO (or residual $AlMe_3$). The anionic amide ligands form N-Al species could increase their catalytic activities [20,29]. The structure around the metal center may account for the different catalytic behaviour of mono N-allyl-substituted catalysts (**29**–**31**)/MAO and bis-(N-allyl-substituted catalysts (**32**–**44**)/MAO.

Titanium, zirconium and vanadium complexes with a 1,2-bis(N-allyl-benzimidazolyl) ligand behave differently depending on the ligand structure. The zirconium complex **34** obtained from 1,2-bis(N-allyl-benzimidazolyl)benzene showed a higher activity than the titanium complex **33**. The vanadium complex **35** is again the most active catalyst in this series (664 [kg PE/mol cat h]) (Fig. 9) and this could be due to very low activation barriers in the various polymerization steps as observed and calculated for the corresponding bis(imino)pyridine complexes [30,31].

The titanium complexes **36**, **39**, and **42** showed activities of 176 [kg PE/mol cat h], 247 [kg PE/mol cat h] and 541 [kg PE/mol cat h]. The same order of activity is observed for zirconium complexes obtained from the same ligand systems (**37**, **40**, **43**) (Fig. 10). This activity order seems to depend on the length of the bridging unit.

The vanadium complexes **38**, **41**, **44** showed different activities depending on the length of the connecting unit as in the case of the titanium complexes obtained from the same ligand system. The N-allyl substituted complexes showed lower activities compared to

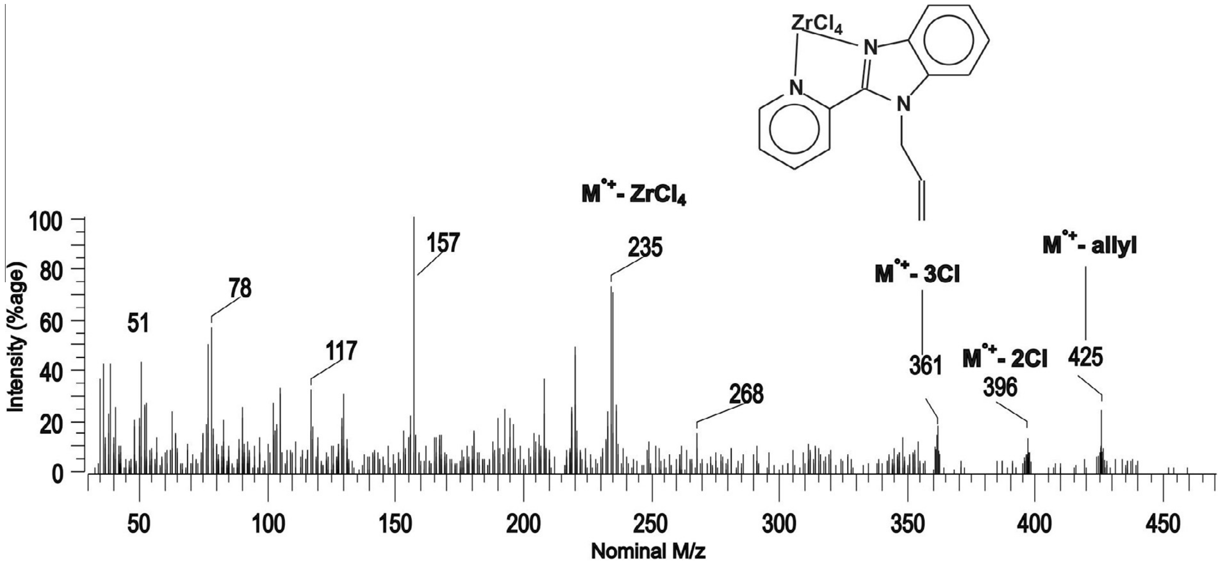

Fig. 6. Mass spectrum of complex **30**.

Table 1
Polymerization results [a] of unsubstituted benzimidazolyl complexes (**13–28**) and the N-allyl-substituted complexes (**29–44**).

Complex no.	Activity (kg PE/ mol cat h)	Al:M	Polymerization temperature (°C)	Mw (g/mol)	PDI
13	307	2500:1	50	1.8×10^5	4.2
14	126	2500:1	50	1.7×10^6	6.3
15	164	2500:1	50	1.1×10^6	13.6
16	n.d.	n.d.	n.d.	n.d.	n.d.
17	252	2500:1	50	1.3×10^6	19.2
18	286	2500:1	50	1.6×10^6	16.4
19	405	2500:1	50	1.6×10^6	9.3
20	208	2500:1	50	1.0×10^6	4.6
21	130	2500:1	50	9.2×10^5	3.8
22	285	2500:1	50	n.d.	n.d.
23	316	2500:1	50	1.1×10^6	8.4
24	172	2500:1	50	1.9×10^6	5.4
25	173	2500:1	50	4.2×10^5	3.2
26	209	2500:1	50	1.3×10^6	16.3
27	53	2500:1	50	n.d.	n.d.
28	231	2500:1	50	1.6×10^6	6.0
29	433	2500:1	50	1.9×10^6	4.4
30	167	2500:1	50	n.d.	n.d.
31	3279	2500:1	50	1.3×10^6	14.2
32	118	2500:1	50	1.2×10^6	7.3
33	98	2500:1	50	n.d.	n.d.
34	209	2500:1	50	1.6×10^6	16.4
35	664	2500:1	50	9.7×10^{65}	7.8
36	176	2500:1	50	1.4×10^6	6.7
37	95	2500:1	50	n.d.	n.d.
38	94	2500:1	50	1.7×10^6	5.9
39	247	2500:1	50	1.9×10^6	4.8
40	78	2500:1	50	n.d.	n.d.
41	115	2500:1	50	1.8×10^6	10.8
42	541	2500:1	50	4.5×10^5	12.4
43	126	2500:1	50	1.3×10^6	9.3
44	134	2500:1	50	1.1×10^6	6.5

[a] All polymerization reactions were carried out in 250 ml pentane with MAO as cocatalyst (Al:M, 2500:1) at 50 °C and 10 bar ethylene pressure, 1 h.

Table 2
Thermal analysis data for representative polymer samples produced with complexes **18, 19, 24, 25, 31, 44**.

Complex no.	T_m (°C)	T_x (°C)	α (%)
18	138.0	117.7	38.0
19	136.7	119.5	33.4
24	137.8	118.6	32.9
25	138.2	121.3	28.3
31	139.9	124.5	21.9
44	137.8	122.2	26.7

T_m = melting temperature, T_x = crystallization temperature, α = degree of crystallinity.

those containing N–H groups (Fig. 11). This can be explained in general by the observed behaviour of all complexes of this type that any factor increasing the electron density on the hetero atom (N, O, S) increases the activity and vice versa.

GPC analyses of the polyethylenes produced with 2-(N-allyl-benzimidazolyl)pyridine, 1,2-bis(N-allyl-benzimidazolyl)benzene, 1,2-bis(benzimidazolyl)ethane, 1,1-bis(N-allyl-benzimidazolyl) methane, and 2,6-bis(N-allyl-benzimidazolyl)pyridine complexes revealed that the symmetric catalysts were capable to produce resins with moderate to very high molecular weights associated with narrow or broad molecular weight distributions. The broadness may arise from the fact that the MAO cocatalyst is undergoing different interactions with the hetero atoms in the catalyst molecule generating different active sites in the activation process [32]. For example, the catalyst **29**/MAO (Fig. 12) produced a resin with $M_w = 1.9 \times 10^6$ g/mol and a polydispersity PD = 4.2 while the catalyst **13/**MAO (derived from unsubstituted benzimidazole)

Table 3
Elemental analysis data of representative organic compounds and complexes.

Compound no.	Calculated			Found		
	C	H	N	C	H	N
1	72.6	4.8	22.6	71.8	4.6	22.4
3	73.3	5.3	21.4	72.9	5.4	21.4
4	77.4	4.5	18.1	77.4	4.5	18.1
7	76.6	5.5	17.9	76.6	5.6	17.8
8	76.7	5.4	17.9	76.7	5.4	17.8
10	77.2	6.4	16.4	77.2	6.4	16.3
20	42.5	3.1	12.4	42.8	2.9	12.1
22	45.8	3.3	13.4	45.5	3.6	13.2
25	44.3	3.0	13.8	44.6	3.2	13.5
30	38.5	2.8	9.0	38.3	2.8	8.9
32	54.7	3.8	12.8	55.1	3.9	12.5
36	45.9	3.8	9.7	45.3	3.9	9.8
41	52.0	4.1	11.6	52.1	4.3	11.3
42	47.6	3.6	11.1	48.2	3.6	11.2

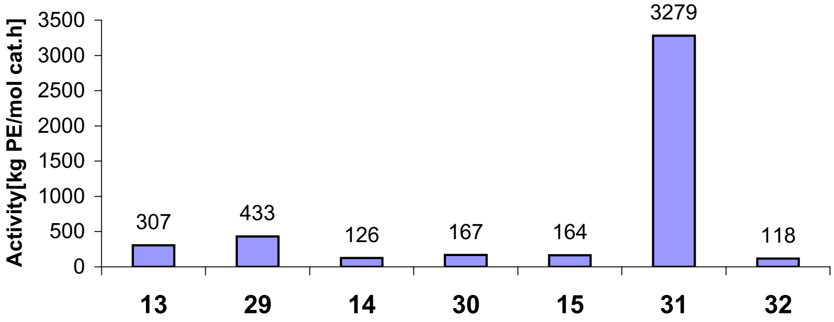

Fig. 7. Polymerization activities of the 2-(N-allyl-benzimidazolyl)pyridine complexes **29–31** compared to the unsubstituted complexes **13–15**.

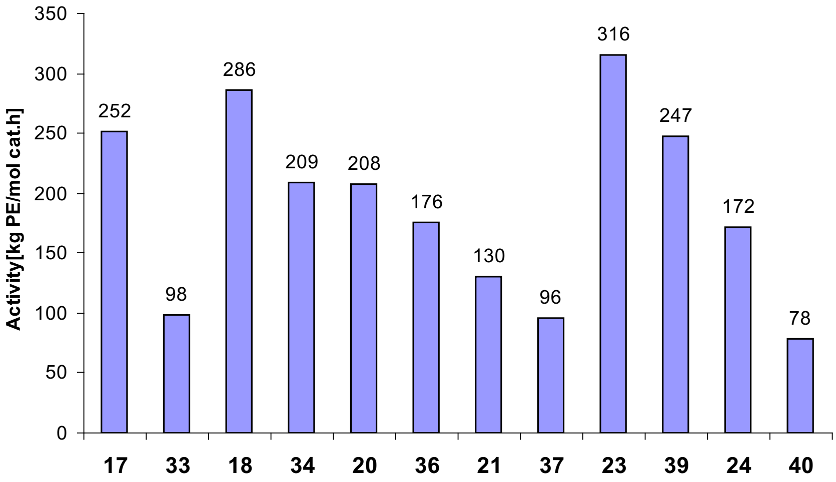

Fig. 8. Effect of the allyl substituent on the polymerization activities of bis(benzimidazolyl) titanium and zirconium complexes.

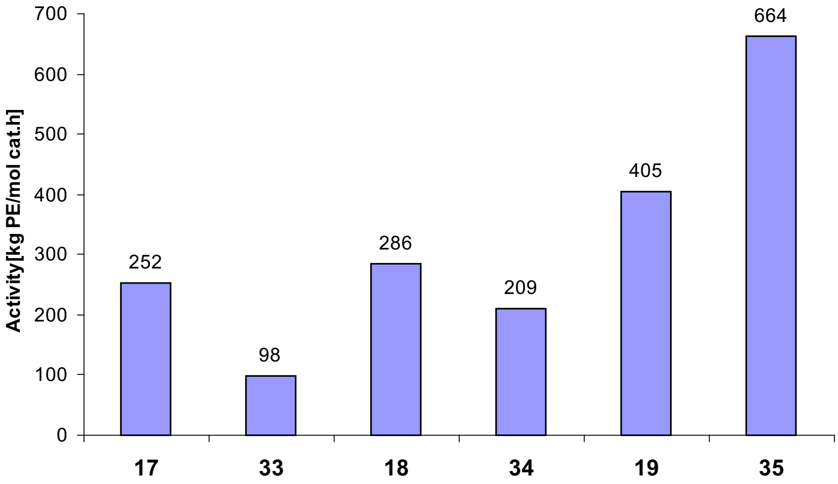

Fig. 9. Activities of 1,2-bis(N-allyl benzimidazolyl) benzene (**33–35**) and 1,2-bis(benzimidazolyl) benzene (**17–19**) complexes.

produced a polyethylene with a molecular weight $M_w = 1.8 \times 10^5$ g/mol and a polydispersity PD = 4.4. The molecular weight and polydispersity of polyethylene obtained with the catalyst **42**/MAO were 4.5×10^5 g/mol and PD = 12.4.

DSC measurements (Table 2) showed that the catalysts produce HDPE with high degrees of crystallinity.

For example, the melting and crystallization temperatures of the polyethylene produced with **31**/MAO was 139.9 and 124.5 °C and the degree of crystallinity $\alpha = 21.9\%$ (Fig. 13).

The melting and crystallization temperatures of the polyethylene produced with **44**/MAO (Fig. 14) was 137.8 and 122.2 °C and the degree of crystallinity $\alpha = 26.7\%$ (Fig. 14).

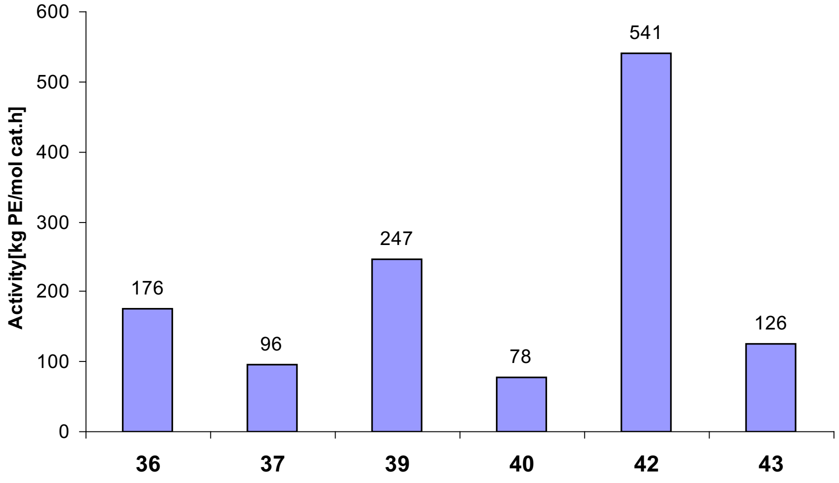

Fig. 10. Activities of 1,2-bis(N-allyl benzimidazolyl)ethane, N-allyl-bis(benzimidazolyl)methane and N-allyl-bis(benzimidazolyl)titanium (**36**, **39**, **42**) and zirconium (**37**, **40**, **43**) complexes.

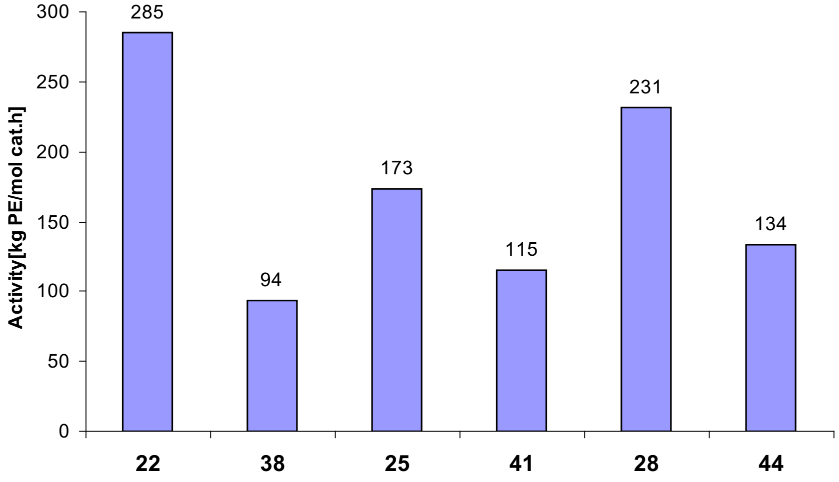

Fig. 11. Effect of the allyl group on the activities of bis-benzimidazolyl vanadium complexes.

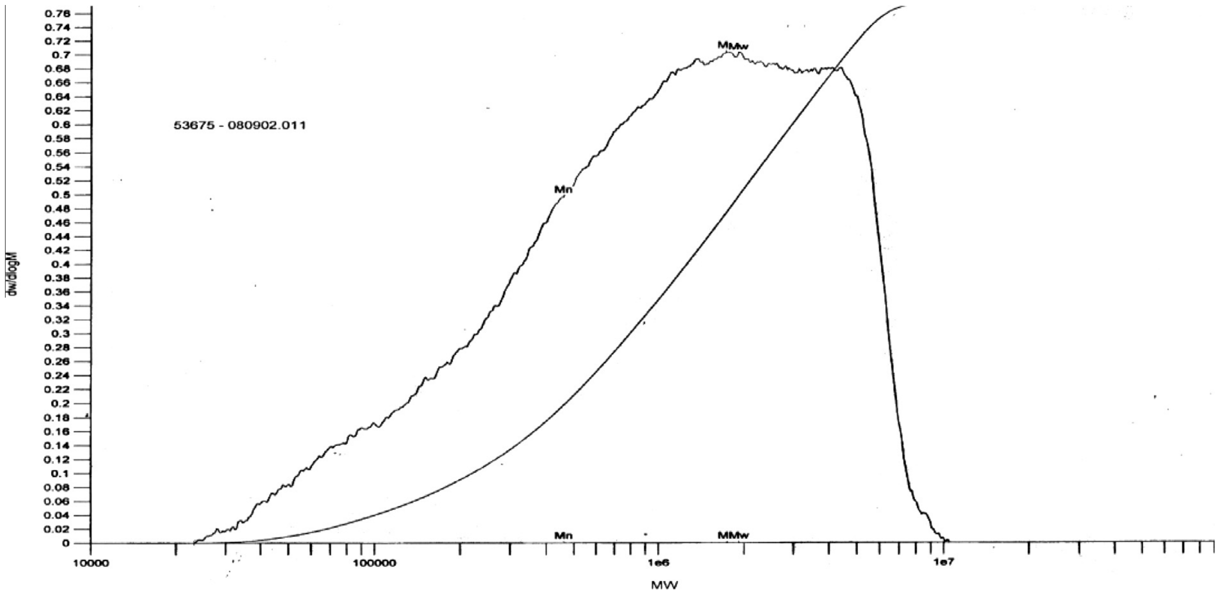

Fig. 12. HT-GPC profile of polyethylene produced with **29**/MAO.

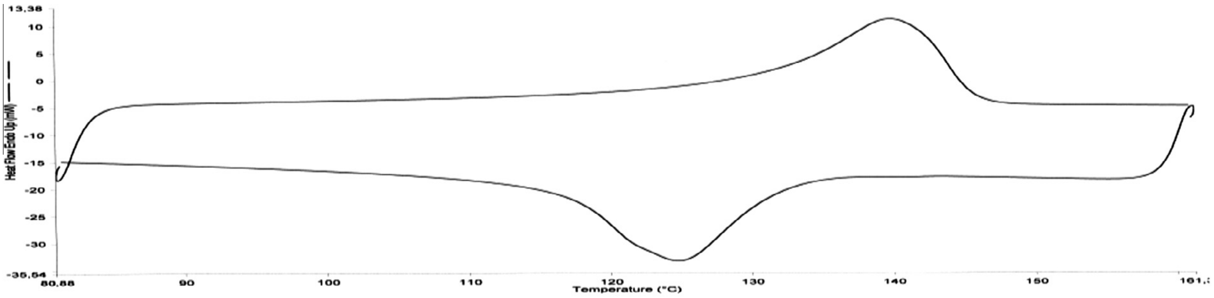

Fig. 13. DSC profile of polyethylene produced with **31**/MAO.

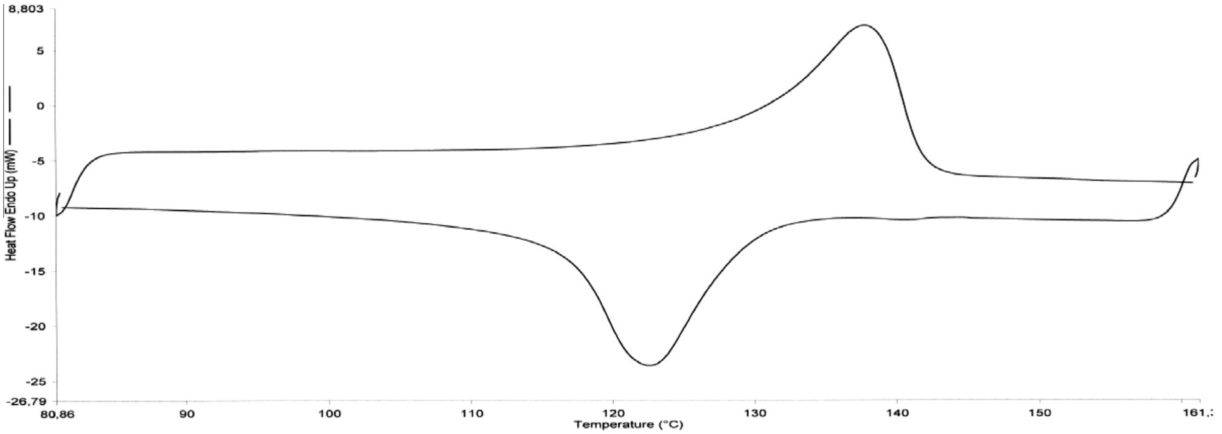

Fig. 14. DSC curve of polyethylene produced with **44**/MAO.

3. Experimental

All experimental work was routinely carried out using Schlenk technique unless otherwise stated. Dried and purified argon was used as inert gas. n-Pentane, diethyl ether, toluene and tetrahydrofuran were purified by distillation over Na/K alloy. Diethyl ether was additionally distilled over lithium aluminum hydride. Methylene chloride was dried with phosphorus pentoxide and calcium hydride. Methanol and ethanol were dried over molecular sieves.

Deuterated solvents ($CDCl_3$, DMSO-d_6) for NMR spectroscopy were stored over molecular sieves (3 Å). Methylalumoxane (30% in toluene) was purchased from Crompton (Bergkamen) and Albemarle (Baton Rouge, USA/Louvain – La Neuve, Belgium). Ethylene (3.0) and argon (4.8/5.0) were supplied by Rießner Company (Lichtenfels). All other starting materials were commercially available and were used without further purification. The titanium and zirconium adducts were synthesized via published procedures [33].

3.1. NMR spectroscopy

The spectrometers Varian Inova 300/400 MHz and Bruker ARX 250 were available for recording the NMR spectra. The samples were prepared under inert atmosphere (argon) and routinely recorded at 25 °C. The chemical shifts in the ^1H NMR spectra are referred to the residual proton signal of the solvent ($\delta = 7.24$ ppm for $CDCl_3$, $\delta = 2.50$ ppm for DMSO) and in ^{13}C NMR spectra to the solvent signal ($\delta = 77.0$ ppm for $CDCl_3$, $\delta = 39.0$ ppm for DMSO-d_6).

3.2. Mass spectrometry

Mass spectra were routinely recorded at the Zentrale Analytik of the University of Bayreuth with a VARIAN MAT CH-7 instrument (direct inlet, EI, E = 70 eV) and a VARIAN MAT 8500 spectrometer.

3.3. Gel permeation chromatography (GPC)

GPC measurements were routinely performed by SABIC Company (Riyadh, Saudi Arabia).

3.4. Elemental analysis

Elemental analyses were performed with a VarioEl III CHN instrument. Calibration compound: acetamide.

3.5. Syntheses

3.5.1. Synthesis of the 1,2-bis(benzoimidazoles)

A diamine compound (0.05 mol) was mixed with a dicarboxylic acid or an acid anhydride (0.025 mol) and the mixture was poured in 50 ml of preheated (100 °C) polyphosphoric acid. The mixture was stirred and heated at 175 °C for 3–5 h. The reaction mixture was then poured in ice cold water and allowed to stand overnight. The precipitate was removed by filtration and washed several times with diluted sodium hydrogen carbonate solution and finally with water. The reaction product was then air dried, weighed and characterized by NMR and mass spectroscopy (Table 4). Representative samples were characterized by elemental analysis (see Table 3).

3.5.2. Synthesis of N-allyl substituted bis-benzoimidazole and benzoimidazolyl pyridine compounds

The general procedure for the reaction of N-allylation was as follows: Benzimidazolyl pyridine (5 g, 25.6 mmol) was dissolved in 10 ml anhydrous DMF. Then K_2CO_3 (1.4 equiv) was added to the solution at room temperature. Shortly afterwards (20 min), allylbromide (25.6 mmol) was added in portions to the reaction mixture. The reaction was stirred at room temperature for two days. The inorganic salt was removed by filtration and rinsed twice

Table 4
NMR and mass spectroscopic data of free ligands **1**–**12** and complexes **13**–**44**.

No.	^{1}H NMR δ (ppm)	^{13}C NMR δ (ppm)	Mass m/z (%)
1	8.69 (d, 1H), 8.29 (d, 1H), 7.95 (t, 1H), 7.59–7.57 (m, 2H), 7.48 (t, 1H), 7.19–7.17 (m, 2H)	151.3, 150.0, 149.1, 138.2, 125.4, 123.2, 122.1	195 $M^{\circ+}$ (100)
2	8.39 (d, 2H), 8.31 (t, 1H), 7.75–7.69 (m, 4H), 7.31–7.24 (m, 4H)	151.4, 148.5, 145.0, 140.1, 135.3, 124.4, 122.9, 122.0, 120.4, 112.6	311 $M^{\circ+}$ (100)
3	7.88 (d, 1H), 7.80 (d, 1H), 7.69 (t, 2H), 7.64 (s, 2H, N–H), 7.61 (m, 4H), 7.26 (m, 4H)	151.6, 137.9, 133.5, 131.9, 129.4, 123.5, 115.5	310 $M^{\circ+}$ (100)
4	7.57 (d, 4H), 7.26 (t, 4H), 3.56 (s, 42H, $2CH_2$)	153.8, 135.4, 124.3, 114.6, 25.4	262 $M^{\circ+}$ (100)
5	12.41 (s, 2H, NH), 7.46 (m, 4H), 7.11 (m, 4H), 4.43 (s, 2H, CH_2)	150.8, 138.4 122.9, 115.4, 29.8	248 $M^{\circ+}$ (100)
6	7.11–6.99 (m, 8H)	156.0, 126.4, 123.8, 116.0	234 $M^{\circ+}$ (100)
7	8.64 (d, 1H), 8.38 (d, 1H), 7.83 (t, 1H), 7.75 (d, 1H), 7.42 (d, 1H), 7.37–7.23 (m, 3H), 6.12–6.02 (m, 1H), 5.52 (d, 2H), 5.11–5.02 (dd, 2H)	150.9, 149.9, 148.8, 142.958, 137.4, 137.0, 133.9, 124.7, 123.9, 123.4, 122.6, 120.1, 116.6, 110.7, 48.1	235 $M^{\circ+}$ (100)
8	8.26 (d, 2H), 7.91 (t, 1H), 7.72 (d, 2H), 7.35 (d, 2H), 7.24 (t, 4H), 5.87–5.80 (m, 22H, 2CH), 5.01 (d, 4H), 4.81 (d, 4H)	150.1, 150.0, 143.0, 138.21, 136.7, 133.2, 125.7, 123.71, 122.9, 120.2, 116.8, 111.1, 47.6	391 $M^{\circ+}$ (100)
9	7.84 (d, 2H), 7.73–7.65 (m, 4H), 7.59–7.47 (m, 4H), 7.19 (t, 2H), 5.71–5.70 (m, 2H), 5.13–4.99 (dd, 4H), 4.60 (d, 4H)	151.2, 132.9, 132.8, 131.8, 130.7, 130.3, 130.2, 129.7, 118.6, 66.2	390 $M^{\circ+}$ (100)
10	7.67 (s, 2H), 7.18–7.17 (m, 6H), 5.86–5.83 (m, 2H, 2CH), 4.98 (d, 4H), 4.76 (s, 4H), 3.48 (s, 42H, $2CH_2$)	154.0, 142.7, 135.4, 132.0, 122.6, 122.2, 119.3, 117.4, 109.7, 45.7, 24.9	342 $M^{\circ+}$ (100)
11	7.58 (d, 2H), 7.50 (d, 2H), 7.20 (t, 4H), 5.99–5.92 (m, 22H, 2CH), 5.14 (d, 4,H), 5.00 (d, 4H), 4.61 (s, 2H, CH)	150.8, 142.9, 135.9, 133.8, 122.8, 122.3, 119.5, 117.6, 111.1, 46.3, 25.6	328 $M^{\circ+}$ (100)
12	7.19 (s, 8H), 5.90–5.84 (m, 2H, CH), 5.25–5.18 (m, 4H), 4.82 (s, 4H)	154.2, 130.6, 126.8, 124.4, 118.5, 115.9, 45.7	314 $M^{\circ+}$ (100)
13	8.93–8.90 (dd, 2H), 8.24 (t, 1H), 7,88–7.85 (dd, 2H), 7.80–7.75 (dd, 1H), 7.61–7.58 (dd, 2H)	151.2, 147.8, 142.8, 139.1, 132.6, 128.3, 127.1, 124.8, 115.1	385 $M^{\circ+}$ (5), 349 $M^{\circ+}$–Cl (10), 312 $M^{\circ+}$–2Cl (5), 276 $M^{\circ+}$–3Cl (15), 243 $M^{\circ+}$–4Cl (5) 195 $M^{\circ+}$–$TiCl_4$ (100)
14	8.79 (d, 1H), 8.50 (d, 1H), 8.08 (t, 1H), 7.71–7.68 (dd, 2H), 7.62–7.59 (dd, 1H), 7.38–7.36 (dd, 2H)	150.8, 148.9, 144.2 138.8, 134.3, 127.3, 125.8, 123.9, 115.5	428 $M^{\circ+}$ (2), 392 $M^{\circ+}$–Cl (15), 355 $M^{\circ+}$–2Cl (20), 320 $M^{\circ+}$–3Cl (5), 284 $M^{\circ+}$–4Cl (5), 195 $M^{\circ+}$–$ZrCl_4$ (100)
15	n.d.	n.d.	352 $M^{\circ+}$ (5), 316 $M^{\circ+}$–Cl (20), 281 $M^{\circ+}$–2Cl (10), 195 $M^{\circ+}$–VCl_3 (100)
17	8.37 (d, 2H), 8.08 (t, 2H), 7.924–7.835 (m, 4H), 7.637–7.625 (m, 4H)	148.2, 134.0, 133.8, 133.6, 126.5, 125.1, 115.4	500 $M^{\circ+}$ (1), 463 $M^{\circ+}$–Cl (2), 428 $M^{\circ+}$–2Cl (3), 394 $M^{\circ+}$–3Cl (5), 357 $M^{\circ+}$–4Cl (2), 310 $M^{\circ+}$–$TiCl_4$ (100)
18	8.28–8.25 (dd, 2H), 7.94 (t, 2H), 7.71–7.67 (m, 4H), 7.45–7.42 (m, 4H)	149.1, 135.0, 132.5, 126.2, 125.4, 115.3, 114.8	543 $M^{\circ+}$ (1), 506 $M^{\circ+}$–Cl (1), 437 $M^{\circ+}$–3Cl (3), 400 $M^{\circ+}$–4Cl (5), 310 $M^{\circ+}$–$ZrCl_4$ (100)
19	n.d.	n.d.	467 $M^{\circ+}$ (1), 430 $M^{\circ+}$–Cl (5), 393 $M^{\circ+}$–3Cl (2), 310 $M^{\circ+}$–VCl_3 (100)
20	7.76–7.70 (m, 4H), 7.50–7.43 (m, 4H), 3.95 (s, 42H, $2CH_2$)	152.5, 132.6, 125.6, 114.6, 24.5	452 $M^{\circ+}$ (5), 416 $M^{\circ+}$–Cl (2), 380 $M^{\circ+}$–2Cl (5), 343 $M^{\circ+}$–3Cl (10), 310 $M^{\circ+}$–4Cl (2), 262 $M^{\circ+}$–$TiCl_4$ (10)
21	7.73–7.71 (m, 4H), 7.45–7.42 (m, 4H), 3.84 (s, 42H, $2CH_2$)	152.7, 133.3, 125.3, 114.7, 24.7	495 $M^{\circ+}$ (2), 458 $M^{\circ+}$–Cl (2), 422 $M^{\circ+}$–2Cl (5), 387 $M^{\circ+}$–3Cl (3), 351 $M^{\circ+}$–4Cl (2), 262 $M^{\circ+}$–$ZrCl_4$ (50)
22	n.d.	n.d.	420 $M^{\circ+}$ (15), 385 $M^{\circ+}$–Cl (15), 343 $M^{\circ+}$–2Cl (10), 310 $M^{\circ+}$–4Cl (2), 262 $M^{\circ+}$–VCl_3 (80)
23	7.52–7.49 (m, 4H), 7.52–7.14 (m, 4H), 4.55 (s, 2H, CH_2)	149.0, 135.4, 124.4, 115.1, 27.5	438 $M^{\circ+}$ (1), 402 $M^{\circ+}$–Cl (2), 367 $M^{\circ+}$–2Cl (2), 248 $M^{\circ+}$–$TiCl_4$ (100)
24	7.63–7.62 (m, 4H), 7.33–7.30 (m, 4H), 4.91 (s, 2H, CH_2)	150.6, 138.7, 122.6, 115.3, 29.6	481 $M^{\circ+}$ (1), 444 $M^{\circ+}$–Cl (2), 407 $M^{\circ+}$–2Cl (1), 370 $M^{\circ+}$–3Cl (2), 336 $M^{\circ+}$–4Cl (1), 248 $M^{\circ+}$–$ZrCl_4$ (100)
25	n.d.	n.d.	406 $M^{\circ+}$ (3), 368 $M^{\circ+}$–Cl (7), 334 $M^{\circ+}$–2Cl (10), 299 $M^{\circ+}$–3Cl (20), 248 $M^{\circ+}$–VCl_3 (100)
26	7.40 (d, 4H), 7.15 (t, 4H)	156.1, 126.6, 123.8, 116.2	425$^{\circ+}$ (2), 352 $M^{\circ+}$–2Cl (2), 317 $M^{\circ+}$–3Cl (10), 234 $M^{\circ+}$–$TiCl_4$ (100)
27	7.18 (d, 4H), 7.04 (t, 4H)	156.2, 126.6, 124.0, 116.2	467$^{\circ+}$ (5), 397 $M^{\circ+}$–2Cl (2), 361 $M^{\circ+}$–3Cl (10), 234 $M^{\circ+}$–$ZrCl_4$ (100)
28	n.d.	n.d.	392$^{\circ+}$ (5), 323 $M^{\circ+}$–2Cl (2), 288 $M^{\circ+}$–3Cl (10), 234 $M^{\circ+}$–VCl_3 (50)
29	8.84 (d, 1H), 8.52 (d, 1H), 8.15 (t, 1H), 7.94–7.92 (m, 1H), 7.89–7.87 (m, 1H), 7.70–7.67 (m, 1H), 7.58–7.54 (m, 2H), 6.09–6.02 (m, 1H, CH), 5.55 (d, 2H, CH_2), 5.20–5.16 (dd, 2H, CH_2)	150.8, 146.5, 144.0, 139.0, 133.8, 132.8, 132.3, 127.7, 127.4, 127.1, 127.0, 119.3, 115.8 114.2, 49.1	347 $M^{\circ+}$–Cl-allyl (7), 312 $M^{\circ+}$–2Cl-allyl (5), 235 $M^{\circ+}$–$TiCl_4$, (100)
30	8.69 (d, 1H), 8.41 (d, 1H), 7.75 (t, 1H), 7.69 (d, 1H), 7.46 (d, 1H), 7.35 (t, 1H), 7.28–7.22 (m, 2H), 6.18–6.01 (m, 1H, CH), 5.50 (d, 2H, CH_2), 5.12–5.02 (dd, 2H, CH_2)	150.9, 146.6, 144.0, 139.0, 134.0, 133.0, 132.4, 127.7 127.4, 127.1, 127.0, 119.5, 115.8, 114.3, 49.2	425 $M^{\circ+}$–allyl (15), 396 $M^{\circ+}$–2Cl (10), 363 $M^{\circ+}$–3Cl (25), 235 $M^{\circ+}$–$ZrCl_4$, (100)
31	n.d.	n.d.	392 $M^{\circ+}$ (1), 356 $M^{\circ+}$–Cl (5), 3321 $M^{\circ+}$–2Cl (5), 315 $M^{\circ+}$–Cl-allyl (5), 235 $M^{\circ+}$–VCl_3, (100)
32	n.d.	n.d.	548 $M^{\circ+}$ (2), 512 $M^{\circ+}$–Cl (5), 477 $M^{\circ+}$–2Cl (5), 441 $M^{\circ+}$–3Cl (2), 430 $M^{\circ+}$–Cl-2allyl (3), 391 $M^{\circ+}$–VCl_3 (100)
33	8.13 (d, 2H), 7.91 (t, 2H), 7.82–7.81 (m, 4H), 7.59–7.56 (m, 4H),	149.7, 133.5, 132.8, 132.2, 131.5, 130.9, 125.7,	580 $M^{\circ+}$ (1), 544 $M^{\circ+}$–Cl (5), 507 M

(*continued on next page*)

Table 4 (*continued*)

No.	^{1}H NMR δ (ppm)	^{13}C NMR δ (ppm)	Mass *m/z* (%)
	5.92–5.85 (m, 2H), 5.22–5.09 (dd, 4H), 4.69 (d, 4H)	118.9, 115.1, 66.3	$^{\circ+}$–2Cl (2), 472 M$^{\circ+}$–3Cl (2), 462 M$^{\circ+}$–Cl-2allyl (3), 390 M$^{\circ+}$–$TiCl_4$ (100)
34	8.15 (d, 2H), 7.90 (t, 2H), 7.85–7.82 (m, 4H), 7.58–7.53 (m, 4H), 5.85–5.72 (m, 2H), 5.24–5.07 (dd, 4H), 4.67 (d, 4H)	149.9, 133.4, 133.0, 132.5, 131.4, 131.3, 125.9, 119.2, 115.0, 66.6	623 M$^{\circ+}$ (2), 587 M$^{\circ+}$–Cl (3), 550 M$^{\circ+}$–2Cl (3), 514 M$^{\circ+}$–3Cl (1), 505 M$^{\circ+}$–Cl-2allyl (5), 390 M$^{\circ+}$–$ZrCl_4$ (100)
35	n.d.	n.d.	550 M$^{\circ+}$ (2), 511 M$^{\circ+}$–Cl (3), 475 M$^{\circ+}$–2Cl (1), 440 M$^{\circ+}$–3Cl (2), 396 M$^{\circ+}$–2Cl-2allyl (3), 390 M$^{\circ+}$–VCl_3 (100)
36	7.80 (d, 2H), 7.71 (d, 2H), 7.43 (t, 4H), 6.15–6.03 (m, 22H, 2CH), 5.78 (d, 42H, $2CH_2$), 5.24 (d, 42H, $2CH_2$), 3.86 (s, 42H, $2CH_2$)	153.2, 133.6, 132.6, 125.1, 125.0, 118.9, 116.3, 115.3, 112.8, 47.0, 23.6	532 M$^{\circ+}$ (1), 495 M$^{\circ+}$–Cl (5), 461 M$^{\circ+}$–2Cl (5), 424 M$^{\circ+}$–3Cl (1), 414 M$^{\circ+}$–Cl-2allyl (2), 342 M$^{\circ+}$–$TiCl_4$ (100)
37	7.92 (d, 2H), 7.81 (d, 2H), 7.56 (t, 4H), 6.11–6.08 (m, 22H, 2CH), 5.36 (d, 42H, $2CH_2$), 5.27 (d, 42H, $2CH_2$), 4.03 (s, 42H, $2CH_2$)	152.5, 132.7, 132.2, 126.1, 125.8, 119.4, 115.3, 114.4, 113.4, 47.4, 23.4	575 M$^{\circ+}$ (2), 505 M$^{\circ+}$–2Cl (3), 468 M$^{\circ+}$–3Cl (1), 423 M$^{\circ+}$–2Cl-2allyl (5), 342 M$^{\circ+}$–$ZrCl_4$ (100)
38	n.d.	n.d.	500 M$^{\circ+}$ (3), 463 M$^{\circ+}$–Cl (5), 429 M$^{\circ+}$–2Cl(2), 418 M$^{\circ+}$–2allyl (3), 342 M$^{\circ+}$–VCl_3 (100)
39	7.85 (d, 2H), 7.81–7.72 (dd, 2H), 7.48 (t, 4H), 6.07–5.92 (m, 22H, 2CH), 5.38–5.27 (dd, 42H, $2CH_2$), 5.21 (d, 42H, $2CH_2$), 5.08 (s, 2H, CH_2)	150.6, 148.1, 135.0, 134.2, 134.0, 133.7, 132.6, 132.4, 125.6, 125.5, 125.3, 125.2, 119.3, 118.5, 117.5, 116.7, 113.2, 113.0, 47.5, 47.2, 24.9	518 M$^{\circ+}$ (3), 482 M$^{\circ+}$–Cl (5), 447 M$^{\circ+}$–2Cl (2), 410 M$^{\circ+}$–3Cl (5), 401 M$^{\circ+}$–Cl-2allyl (5), 328 M$^{\circ+}$–$TiCl_4$ (100)
40	7.85 (d, 2H), 7.75–7.72 (dd, 2H), 7.49 (t, 4H), 6.03-5.98 (m, 22H, 2CH), 5.34–5.27 (dd, 42H, $2CH_2$), 5.22- (s, 42H, $2CH_2$), 5.19 (s, 2H, CH_2)	150.6, 148.2, 135.2, 134.2, 134.0, 133.8, 132.6, 132.4, 125.5, 125.3, 125.3, 125.0, 119.3, 118.5, 117.5, 116.8, 113.1, 113.1, 47.4, 47.2, 24.9	561 M$^{\circ+}$ (3), 525 M$^{\circ+}$–Cl (5), 454 M$^{\circ+}$–3Cl (2), 407 M$^{\circ+}$–2Cl-2allyl (5), 328 M$^{\circ+}$–$ZrCl_4$ (100)
41	n.d.	n.d.	485 M$^{\circ+}$ (2), 449 M$^{\circ+}$–Cl (3), 415 M$^{\circ+}$–2Cl (2), 367 M$^{\circ+}$–2Cl-2allyl (5), 328 M$^{\circ+}$–VCl_3 (100)
42	7.36–7.33 (m, 4H), 7.25–7.21 (m, 4H), 5.98–5.88 (m, 22H, 2CH), 5.22–5.16 (m, 42H, $2CH_2$), 4.81–4.79 (m, 42H, $2CH_2$)	154.3, 132.2, 127.1, 124.4, 117.7, 116.5, 45.4,	467 M$^{\circ+}$–Cl (10), 433 M$^{\circ+}$–Cl –allyl (10), 397 M$^{\circ+}$–3Cl (10), M$^{\circ+}$–4Cl (15), 317 M$^{\circ+}$–$TiCl_4$ (20)
43	7.30–7.29 (m, 4H), 7.24–7.21 (m, 4H), 5.99–5.90 (m, 22H, 2CH), 5.23–5.19 (m, 42H, $2CH_2$), 4.85–4.79 (m, 42H, $2CH_2$)	154.0, 132.5, 126.6, 124.8, 118.1, 116.2, 45.7,	547 M$^{\circ+}$ (2), 511 M$^{\circ+}$–Cl (5), 476 M$^{\circ+}$–2Cl (5), 440 M$^{\circ+}$–3Cl (3), 314 M$^{\circ+}$–$ZrCl_4$ (20)
44	n.d.	n.d.	472 M$^{\circ+}$ (6), 400 M$^{\circ+}$–2Cl (5), 363 M$^{\circ+}$–3Cl (3), 314 M$^{\circ+}$–VCl_3 (15), 278 M$^{\circ+}$–3Cl-2allyl (20)

[*] Complex **16** was not prepared.

with dichloromethane. The solution was poured into water and extracted with dichloromethane (2 × 50 ml). The combined organic layers were washed with brine, dried over anhydrous sodium sulfate, filtered, and concentrated in vacuo resulting in a viscous oil. Addition of water resulted in the formation of the product in 85% yield. Other N-allyl substituted compounds were prepared similarly. The products were characterized by NMR and mass spectroscopy (Table 4). Representative samples were characterized by elemental analysis (Table 3).

3.5.3. General procedures for the synthesis of the complexes

3.5.3.1. Titanium complexes. To 0.87 g, (2.6 mmol) $TiCl_4(THF)_2$ in dichloromethane was added 2.6 mmol of the solid heterocycle. The reaction mixture was stirred over night at room temperature and filtered. The residue was washed several times with dichloromethane and pentane and dried in vacuo and weighed. The products were characterized by NMR and mass spectroscopy (Table 4). Representative samples were characterized by elemental analysis (Table 3).

3.5.3.2. Zirconium complexes. To 0.45 g (1.2 mmol) $ZrCl_4(THF)_2$ in dichloromethane was added 1.2 mmol of the free ligand. The reaction mixture was stirred over night at room temperature, the reaction product was filtered and washed several times with dichloromethane and pentane, dried in vacuo and weighed. The products were characterized by NMR and mass spectroscopy (Table 4). Representative samples were characterized by elemental analysis (Table 3).

3.5.3.3. Vanadium complexes. To 0.41 g (2.6 mmol) VCl_3 in ether was added 2.6 mmol of the ligand. The reaction mixture was stirred over night at room temperature. The product was filtered and washed several times with ether and pentane, dried in vacuo and weighed. Representative samples were characterized by elemental analysis (Table 3).

3.6. Polymerization of ethylene in a 1 L Büchi autoclave

An amount of 2–5 mg of the desired complex was suspended in 5 ml of toluene. Methylalumoxane (30% in toluene) was added resulting in an immediate color change. The mixture was transferred to a 1 l Schlenk flask filled with 250 ml n-pentane. This mixture was transferred to a Büchi laboratory autoclave under inert atmosphere and thermostated. An ethylene pressure of 10 bar was applied for one hour. The obtained polymer was filtered over a frit, washed with diluted hydrochloric acid, water, and acetone, and finally dried in vacuo.

4. Conclusions

The N-allyl functionalized complexes offer a whole platform of applications in catalytic ethylene polymerization and they are good candidates for single-reactor bimodal/multimodal polyethylene technology. The production of bimodal or multimodal resins can be explained with the existence of different active sites in the polymerization process caused by different interactions of the MAO cocatalyst with the hetero atoms in the catalyst. In addition, the alkenyl function in the catalyst allows self-immobilization without an external support. Because of these features such catalysts belong into the category “intelligent catalysts”.

Acknowledgements

We thank SABIC company (Riyadh, Saudi Arabia) for GPC measurements and University of Juba (Khartoum, Sudan) for the financial support of H.A.E. for the first year.

References

[1] W. Kaminsky, M. Fernandes, Polyolefins J. 2 (2015) 1.
[2] C. Redshaw, Y. Tang, Chem. Soc. Rev. 41 (2012) 4484.
[3] M.C. Baier, M.A. Zuideveld, S. Mecking, Angew. Chem., Int. Ed. 53 (2014) 9722.
[4] W. Kaminsky (Ed.), Polyolefins: 50 years After Ziegler and Natta, 257, Springer, Adv. Polymer Science, 2013, p. 14.
[5] H.G. Alt, Polyolefins J. 2 (2015) 17.
[6] H.G. Alt, Macromol. Symp. 173 (2001) 65.
[7] B. Peifer, W. Milius, H.G. Alt, J. Organomet. Chem. 553 (1998) 205.
[8] H.G. Alt, J. Chem. Soc., Dalton Trans. (1999) 1703.
[9] H.G. Alt, J. Chem. Soc., Dalton Trans. (2005) 3271.
[10] H.G. Alt, C. Görl, in: John R. Severn, John C. Chadwick (Eds.), Tailor-Made Polymers via Immobilization of Alpha-Olefin Polymerization Catalysts, Wiley-VCH, 2008, pp. 305–326.
[11] H. Alshammari, H.G. Alt, Jordan J. Chem. 9 (2014) 34.
[12] H.G. Alt, R. Ernst, Inorg. Chim. Acta 350 (2003) 1.
[13] C. Görl, H.G. Alt, J. Organomet. Chem. 692 (2007) 5727.
[14] H. Alshammari, H.G. Alt, Jordan J. Chem. 9 (2014) 110.
[15] H. Alshammari, H.G. Alt, Polyolefins J. 1 (2014) 107.
[16] H.A. Elagab, H.G. Alt, Eur. Polym. J. 71 (2015) 85.
[17] H.A. Elagab, H.G. Alt, Inorg. Chim. Acta 428 (2015) 100.
[18] Y. Kikugawa, Synthesis (1981) 124.
[19] X. Xu, Z. Xi, W. Chen, D. Wang, J. Coord. Chem. 60 (2007) 2297–2308.
[20] W. Zhang, W.-H. Sun, S. Zhang, J. Hou, K. Wedeking, S. Schultz, R. Fröhlich, H. Song, Organometallics 25 (2006) 1961.
[21] L. Wang, M.M. Joullie, J. Am. Chem. Soc. 79 (1957) 5703.
[22] C. Rai, J.B. Braunwarth, J. Org. Chem. 26 (1961) 3434.
[23] D.J. Brondani, D.R. De Magalhaes, M.P. De Farias, F.R. Souza, F.F. Barbosa, A.C.L. Leite, Tetrahedron Lett. 48 (2007) 3919.
[24] M. Bochmann, L.M. Wilson, J. Chem. Soc., Chem. Commun. 21 (1986) 1610.
[25] M. Seitz, PhD Thesis, University Bayreuth, 2004.
[26] M. Seitz, C. Görl, W. Milius, H.G. Alt, Jordan J. Chem. 3 (2008) 109–145.
[27] R.F. Jordan, C.S. Bajgur, W.E. Dasher, A.L. Rheingold, Organometallics 6 (1987) 1041.
[28] M. Seitz, W. Milius, H.G. Alt, J. Mol. Catal. A: Chem. 261 (2007) 246.
[29] A.C. Möller, R. Blom, R.H. Heyn, O. Swang, J. Kopf, T. Seraidaris, J. Chem. Soc., Dalton Trans. (2006) 2098.
[30] A.C. Möller, R. Blom, O. Swang, A. Hannisdal, E. Rytter, J.A. Stovneng, T. Piel, J. Phys. Chem. 112 (2008) 4074.
[31] D.S. McGuinness, P. Wasserscheid, D.H. Morgan, J.T. Dixon, Organometallics 24 (2005) 552.
[32] H.G. Alt, R. Ernst, J. Mol. Catal. A: Chem. 195 (2003) 11.
[33] L.E. Manzer, Inorg. Synth. 21 (1982) 135.